

MAGNETIC FIELD EFFECTS ON CONVECTION AND SOLIDIFICATION IN NORMAL AND MICROGRAVITY

Ben Q. Li^{*} and H. C. de Groh III²

¹School of Mechanical and Materials Engineering, Washington State University, Pullman, WA

²NASA Glenn Research Center, Cleveland, OH 44135

Abstract

It has been well understood that convective flows induced by g-jitter forces associated with spacecraft are responsible for defects formation and irregularity in product quality during melt growth of single crystals in microgravity. This research is concerned about numerical simulations and experimental measurements for the purpose of developing a fundamental understanding of the g-jitter induced fluid flows and their effects on solidification in microgravity with and without the presence of additional damping forces that are derived from the applied DC magnetic fields. The numerical models include both 2-D and 3-D transient fluid flow, heat transfer, mass transfer and solidification under the combined action of g-jitter and magnetic fields. Numerical simulations using both the 2-D and 3-D models are conducted for both idealized, synthesized and real g-jitter forces, and 2-D simulations are tested against the experimental measurements taken on the thermal oscillator. 2-D solidification models have also been developed and simulations are conducted. Results show that the numerical model predictions compare well with the measurements. Analysis of these results illustrates that an applied magnetic field can have a drastic influence on the convective flows induced by g-jitter and can be particularly useful to suppress the effects resulting from the spiking of g-jitter signatures, which are considered the most detrimental effects on quality of crystals grown in space. Work in progress includes developing 3-D numerical models for solidification phenomena with the presence of both g-jitter and magnetic fields and measurements of flow fluid and its effect on solidification in both transparent fluid and low melting point melts to verify numerical predictions.

I. Introduction

Microgravity and magnetic damping are two mechanisms applied during the melt growth of semiconductor or metal crystals to suppress buoyancy driven flow so as to improve macro and micro homogeneity of the crystals. As natural convection arises from gravity effects, microgravity offers a plausible solution to reduce the convective flow. However, recent flight experiments indicate that residual accelerations during space processing, or g-jitter, can cause considerable convection in the liquid pool, making it difficult to realize a diffusion controlled growth, as originally intended, when experiments were conducted in microgravity [1]. Further studies showed that g-jitter is a random phenomenon associated with microgravity environment and has both steady state and transient effects on convective flow. Since molten metals and semiconductor melts are electrically conducting, magnetic damping may be explored to suppress the unwanted g-jitter induced convection during solidification [2].

The objective of this work is to further develop and verify numerical capabilities in support of microgravity materials science programs involving the use of magnetic fields to dampen convection. The objectives

Keywords: magnetic damping, g-jitter induced convection, solidification, electromagnetic levitation, electrostatic levitation

* Corresponding author email: li@mme.wsu.edu

of the proposed research are to (1) conduct measurements of oscillating melt flows in physical models, and to verify and refine the melt flow model developed for g-jitter induced flows against the measured data; (2) assess the effect of oscillating convective flows on solidification in a microgravity environment through numerical modeling and ground-based laboratory measurements; and (3) understand and quantify the effect of convective flow enhancement in a DC magnetic field, whose main action has so far been understood to provide damping effects on convection. Significant progress has been made in achieving the objective and research results are presented in several publications [3-17]. Below we discuss some crucial results, some of which are still being further analyzed.

II. Experimental Measurements

A physical model using transparent fluids such as water and SCN has been established to study the oscillating flow induced by oscillating thermal gradient and the effect of fluid flow on solidification. The detailed experimental setup is shown in Figure 1. The system consists of three computers, a laser generator, a CCD camera, a test cavity cell, a heat stripe, two isothermal water baths and an expansion board. The function of the computer on the left is to collect temperature data and to control the shutter of the CCD camera for flow visualization and PIV measurements. Two integrated circuit boards (CIO-DAS 1402/16 and CIO-CRT05, both from ComputerBoards Inc.) were installed in the computer, with the former for analog/digital conversion, and the later the control of shutter speed of the CCD camera. The middle computer is to control the heat stripe mounted on the test cell. It uses its own counter board and sends signals to the AC power generator (Model XHR 150-7 from XANTREX Com.) to generate the oscillating electrical wave required to produce an oscillating temperature field. The computer on the right is a dual processor PC, designed for data intensive computations for image processing. It combines image capturing and image processing into one unit. Its high speed and big memory makes it possible to save the images as fast as needed for our applications. This computer is synchronized with that on the left to obtain the temperature and velocity at the same time.

The main part of the system is a rectangular cavity with a dimension of 1.80cm×2.03cm×15.0cm. The length is 6 times more than the height and width to eliminated the 3-D effect. The top and bottom walls were made of 1.27cm thick acrylic. Also some polystyrene was glued on these plates for insulation purpose. The two side walls were made of 3.16mm thick grade copper in order to get good heat conduction. To prevent the copper side walls from reflecting laser's light, black layer was painted on the inside surface of the side walls.

Before any measurements were taken, the water was allowed to flow through the thermobaths (or thermomixers) for about half an hour to establish a steady state. Then the required frequency was turned on and the heater was activated, while the temperature along two side walls was monitored. Various testing cases showed that after 5~6 cycles, the temperature and the fluid flow reached a quasi-steady harmonic motion. In our case, the lowest frequency used was about 0.01Hz. That means both the flow and temperature become quasi-steady within 10 minutes, or 6 cycles. To ensure the fully oscillated condition so as to collect data for comparison with the numerical modeling, it was allowed to run more than 30 minutes before starting to collect temperature data and capture the images.

III. Comparison of Simulations with Experiments

We have developed both 2-D and 3-D numerical models for the transient fluid flow, heat transfer and solutal transport under the influence of g-jitter with and without the presence of an external magnetic

field. The model development was based on the finite element solution of the transport equations with the Lorentz forces as a momentum source and entails the modification of our in-house finite element fluid flow and heat transfer code. The numerical models were further tested against the analytical solution for the application of magnetic damping to suppress the g-jitter induced convective flows, and excellent agreement exists between the two approaches [4,5]. With the numerical models, extensive simulations have been carried out [6-16].

Experiments were conducted for various configurations and different conditions. As noted in previous studies, for space applications the low frequency has the most important effect. Numerical simulations of g-jitter driven convection show that the most detrimental effects come from the frequency range of 0.01 to 0.5 Hz, which is the approximate range of studies. To produce an oscillating thermal gradient, the temperature at one wall is fixed and that at the opposite is oscillated, with the mean temperature being the fixed wall temperature. This implementation gave a very stable wall temperature oscillation after a short transient period.

Figure 2 shows the oscillation of convection patterns, along with the computed results for the oscillation frequency of 0.025 Hz. As the flow is transient and evolves in time, only some of the snap shot pictures can be presented here. These snap shots of the transient convection reveal some of the very essential features of the convection in the system. Examination of these figures illustrates that both the experimental measurements and the numerical simulations are in excellent agreement. Both the measured and computed results show that the liquid convection in the cell responds to the temperature changes in time. A large convection cell is developed initially, circulating down along the cold wall and moving upward along the hot wall, as shown in Figure 2a1 – a3. The icon of this large flow cell is located closer to the hot wall as well to satisfy the mass conservation across the liquid pool. It is noticed that the flow near the hot shows a high velocity magnitude and it becomes weak near the cold at the instant. Near the lower corner of the cold wall, a smaller, weak and anti-rotating flow eddy develops and appears to contribute to the weakening of the convection along the cold wall.

The convective flow field continues to evolve in response to the temperature change in time. The weaker and smaller cell appearing at the low corner of the liquid pool, as shown in Figure 2a3, continues to grow in strength and invade in to the territory of the large cell. As the temperature decreases at the hot wall below the cold temperature, the initially small cell takes the entire liquid pool, reversing the global flow structure completely. This is clearly seen in Figures 2c3, where the temperature at the hot wall is actually reduced below the cold wall temperature, thereby causing the flow reversing. There appears to be a rather weaker and small flow cell developing at the upper corner near the cold wall. The comparison of measured and calculated velocities at two specific locations, as evolving in time, is illustrated in Figure 3. Evidently, there exists gratifying agreement between the experimental measurements and numerical model predictions. Analyses of the measured and computed results show that there exists a phase angle between the temperature variation and the flow oscillation and this phase angle depends on many factors. The angle is a function of location, the applied temperature and the oscillating frequency, which confirms our early studies [4-7].

Early analyses have suggested that the perturbations of high frequencies produce small or negligible effects on convection and solutal striation but offered no physical explanation. That the high frequency component does not affect the flow motion is confirmed by our experimental measurements and

corresponding numerical simulations, as shown in Figure 4, for an oscillating frequency of 0.1 Hz and beyond. Here it is apparent that the convection in the liquid is no longer oscillating, despite the oscillating temperature gradients applied on the two opposite walls. For this case, both the experimental measurements and numerical simulations depict two anti-rotating, steady state flow cells, equal in size and strength, which are recirculating in the entire liquid pool. To explore the reasons how the frequency truly affects the convection, a set of numerical simulations, using the finite element model verified through the experimental measurements described above. These simulated results show that, while temperature is forced to oscillate at the hot wall to establish a oscillating temperature gradient cross the liquid pool, the oscillating is largely confined in a very thin layer of the wall, when the oscillating frequency is set at 0.1 Hz. For this case, the temperatures at both the hot and cold walls are seen to be higher than that at the center portion of the liquid pool, while still maintaining the overall heat balance.

From the experimental measurements and computed results for other conditions, it is found that the convection pattern and flow oscillation is a strong function of applied frequency and is also dependent upon the orientation of the liquid cell with respect to gravity. The orientation effects are shown in a set of snap shots of the measured and computed results at various instants for a 45° tilted configuration, where gravity points downwards (see Figure 5). Clearly, the measured and computed results for this configuration are once again in excellent agreement for both flow patterns and velocity magnitudes. The oscillating flow structures are very similar to those presented above when gravity is perpendicular to the temperature gradient, in response to the time evolution of the thermal environment. However, both the measured and computed results show some subtle and yet important differences between the two configurations, as contrasted in Figure 5cs and Figure 2bs or Figure 5ds and Figure 2cs. In Figure 5cs, the flow field is characterized by three flow cells, with two large ones, approximately equal in size and strength, occupying the entire liquid pool and a small one appearing at the upper corner of the hot wall. In contrast, for the same temperature gradient, there are only two cells, with the large one taking the majority portion of the liquid pool and the smaller barely noticed at the upper corner of the cold wall. The maximum velocities are also different for two cases.

IV. 2-D Solidification Model and Numerical Simulations

Solidification models for 2-D geometries have also been developed. Both fixed grid and moving methods have been applied to develop the models and the results obtained using both methods are the same as they should. With the above experimental system, measurements were made to determine the fluid flow field and its effect on solidification morphologies. The experiments were conducted using the SCN fluid, which has been frequently used in microgravity research community. These measured results are compared with numerical predictions. Two of these comparisons are given in Figure 6 for the cavity tilted at an angle of 45° with gravity field. To ensure consistent comparison with experimental measurements, the numerical results are obtained using the fixed grid method. Apparently, the model predictions and experimental measurements are in good agreement.

With the 2-D model developed and verified as described above, numerical simulations were further carried out to study the convection induced by g-jitter and its effect on solidification for a system being considered for space flights.

Under an idealized microgravity condition, the gravity level is $10^{-6}g_0$. This condition may be obtained when the space vehicle follows the orbit perfectly without disturbances. Numerical simulations were

carried out for this condition without an imposed magnetic field. The calculations will serve a dual purpose. The results are useful in helping to gain physical insight into the steady state behavior of the system. They also provide the initial condition for the dynamic behavior of the system when g-jitter effects set in. To consider the worst scenario, the gravity is assumed to be oriented perpendicular to the growth direction, which represents the worst scenario case. The computed results show that the flow field is dominated overwhelmingly by the growth velocity, and the thermal and solutal gradient induced convective flow recirculation is small. These results are consistent with those obtained earlier from a simplified melt flow system where solidification was not considered, confirming that these simplified models indeed provide a good approximation to the melt flows under more realistic growth conditions, as they are intended to. Temperature distributions in the growth system are largely controlled by thermal conduction, which is a direct result of small Prandtl number for the system being studied. The solute distribution, on the other hand, appears to experience a slight distortion, which results from the small convection induced by the microgravity force.

Detailed analysis shows that for this case, the solute distribution has a striation of about 7%, measured by $(C_{\max} - C_{\min})/C_{\text{average}}$ along the solid-liquid interface. This concentration non-uniformity will affect the melting temperature and thus the system performance. Figure 7 compares the computed results of concentration and the normalized melting temperature distributions along the solid-liquid interface, and the solidification interface position for the system with and without taking into account the concentration effect on the melting temperature. It transpires that with the concentration effects considered, the melting temperature is no longer a constant, which results in a noticeable change in the solidification interface position. It is thus important to include the concentration effect on the melting temperature.

Numerical simulations have been carried out to study the effect of both idealized single frequency g-jitter and real g-jitter on fluid flow and solidification with and without the presence of an applied magnetic field. In a real space environment, g-jitter perturbations are random in direction, orientation and magnitude. While the studies on the single frequency effects are of great value in helping to understand the fundamentals governing the thermally induced oscillating flows, information on the fluid flow and mass transfer in a real g-jitter environment is of both fundamental and practical significance. Numerical simulations were made using the real g-jitter data, taken from the accelerometers aboard on Space Shuttle during a typical space flight. To assess the magnetic effects, calculations were made with and without the presence of an applied magnetic field. The computed results included the evolution of the flow velocity components, the interface shapes and the concentration striation along the interface and some of these calculated results are given in Figures 8 and 9. These results show that in the absence of an applied magnetic field, the velocities experience sharp spikes, in response to the change of g-jitter forces. These spiking velocities cause a strong solute variation in the melt, whence the defects are incorporated into the crystals in a random fashion. This is exactly what is observed in space grown crystals. Inspection of these results clearly indicates that the applied magnetic field can be applied effectively to suppress the spiking velocities, thereby reducing the variation of the concentration field, as one might have deduced from the single frequency simulations discussed above. The analysis of the computed results suggests that the applied magnetic field does not affect influence the solid-liquid interface. However, it substantially suppresses the concentration variation along the interface (see Figure 9). It is noteworthy that with a moderate magnetic field (0.5 Tesla), the concentration non-uniformity along the interface is almost entirely smoothed out.

V. Work In Progress

The work in progress involves extensive experimental measurements and numerical simulations to obtain more information that will help to enhance our fundamental understanding of magnetic damping effects on g-jitter induced flow and solidification phenomena in space processing systems and to help design damping facilities for microgravity applications. Numerical simulations will be continued to study magnetic damping of g-jitter flows and solutal striation and to quantify the effects of the field strength and direction, and the g-jitter frequency, orientation and amplitude, on the convective flows and solutal distribution and evolution in solidification systems. 3-D model for solidification phenomena is being developed, which will allow us to address both spatial and temporal effects more accurately. Ground-based measurements of oscillating flows and their effects on solidification will be conducted in the physical. The physical measurements will be compared with the numerical model predictions.

VI. References

1. Lehoczky, S., Szofran, F. R. and Gillies, D. C. "Growth of solid solution single crystals." Second United States Microgravity Payload, Six Month Sciences Report, NASA MSC (1994).
2. B. Q. Li, "G-jitter induced flows in a transverse magnetic field." *Int. J. Heat & Mass Trans.*, Vol. 39, No. 14, pp. 2853-2860 (1996).
3. M. L. Higgins, "PIV study of oscillating natural convection flow within a horizontal rectangular enclosure." WSU MS Thesis (2000).
4. Y. Shu, B. Q. Li and H. C. de Groh, "Numerical study of g-jitter induced double diffusive convection in microgravity", *Numerical Heat Transfer B: Application*, Vol. 39, No. 3, 2001, 245-265.
5. B. Q. Li, "Stability of modulated-gravity induced thermal convection in a magnetic field", *J. of Physics Review E*, Vol. 63, 2001, pp. 041508-1:041508-9.
6. B. Pan, D. Y. Shang, B. Q. Li and H. C. de Groh "Magnetic damping effects on g-jitter driven melt convection and mass transfer in microgravity", *Int. J. Heat & Mass Transf.*, Vol. 45, pp. 125-144, 2002.
7. Y. Shu, B. Q. Li and H. C. de Groh, "Magnetic damping of g-jitter induced double diffusive convection in microgravity", *Numerical Heat Transfer A: Application*, in print.
8. B. Q. Li and R. He, "Computational modeling of electrodynamic and transport phenomena under terrestrial and microgravity conditions," *Int. J. of Applied Electromagnetics & Mech.*, accepted.
9. K. Li and B. Q. Li, "Effects of magnetic fields on g-jitter induced convection and solute striation during space processing of single crystals," *Int. J. Heat & Mass Transf.*, submitted.
10. K. Li and B. Q. Li, "Numerical analyses of g-jitter induced convection and solidification in magnetic fields," *J. thermophysics and heat transfer*, submitted.
11. J. Honda, C. Zhang, B. Q. Li and H. C. de Groh, "A 3-d model for magnetic damping of g-jitter induced convection and solutal transport in a simplified Bridgmann configuration," in *Proceedings of the ASME Heat Transfer Division*, Nov. 2001, New York, Paper #: IMECE2001/HTD-24291, 2001, pp. 1-18.
12. B. Q. Li, "Computational modeling of electrodynamic and transport phenomena in materials processing systems under terrestrial and microgravity conditions," the 10th International Symposium in Applied Electromagnetics and Mechanics, Tokyo, Japan, May 13-16, 2001, pp. 471-472.
13. W. Song, Govindaraju, B. Q. Li and Y. Pang, "Mathematical modeling of melt flow and heat transfer during electromagnetic processing of light metals," the 4th International Conference on Advanced Materials Processing, Hawaii, Dec., 2001, pp. 341-344.

14. Y. Shu, M. Higgins, B. Q. Li and B. Ramaprian, "A PIV study of natural convection induced by oscillating thermal gradients," *Flow visualization*, ASME 2002 Annual Meeting, New Orleans, LA, accepted.
15. K. Li, B. Q. Li and H. C. de Groh, "Finite element analyses of g-jitter induced convection and solidification in magnetic fields," Computational Heat Transfer in reduced gravity, ASME 2002 Annual Meeting, New Orleans, LA, accepted.
16. Y. Shu, K. Li, B. Q. Li and h. C. de Groh, "Fluid flow motion and solidification under combined action of magnetic fields and microgravity," TMS annual meeting, March, 2003, Sa Diego, submitted.

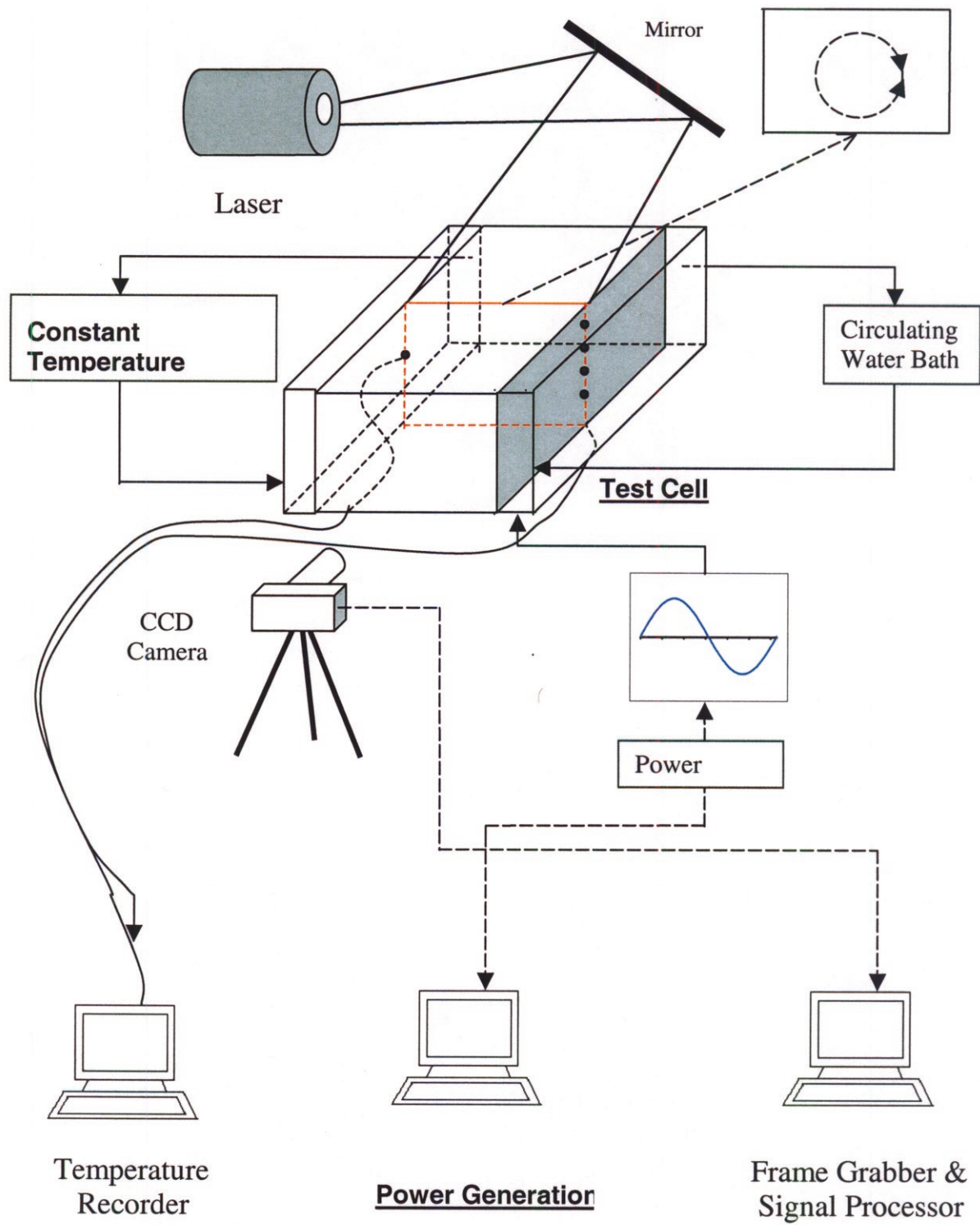


Figure 1. Schematic of the experimental setup for the PIV measurement of thermally induced oscillation.

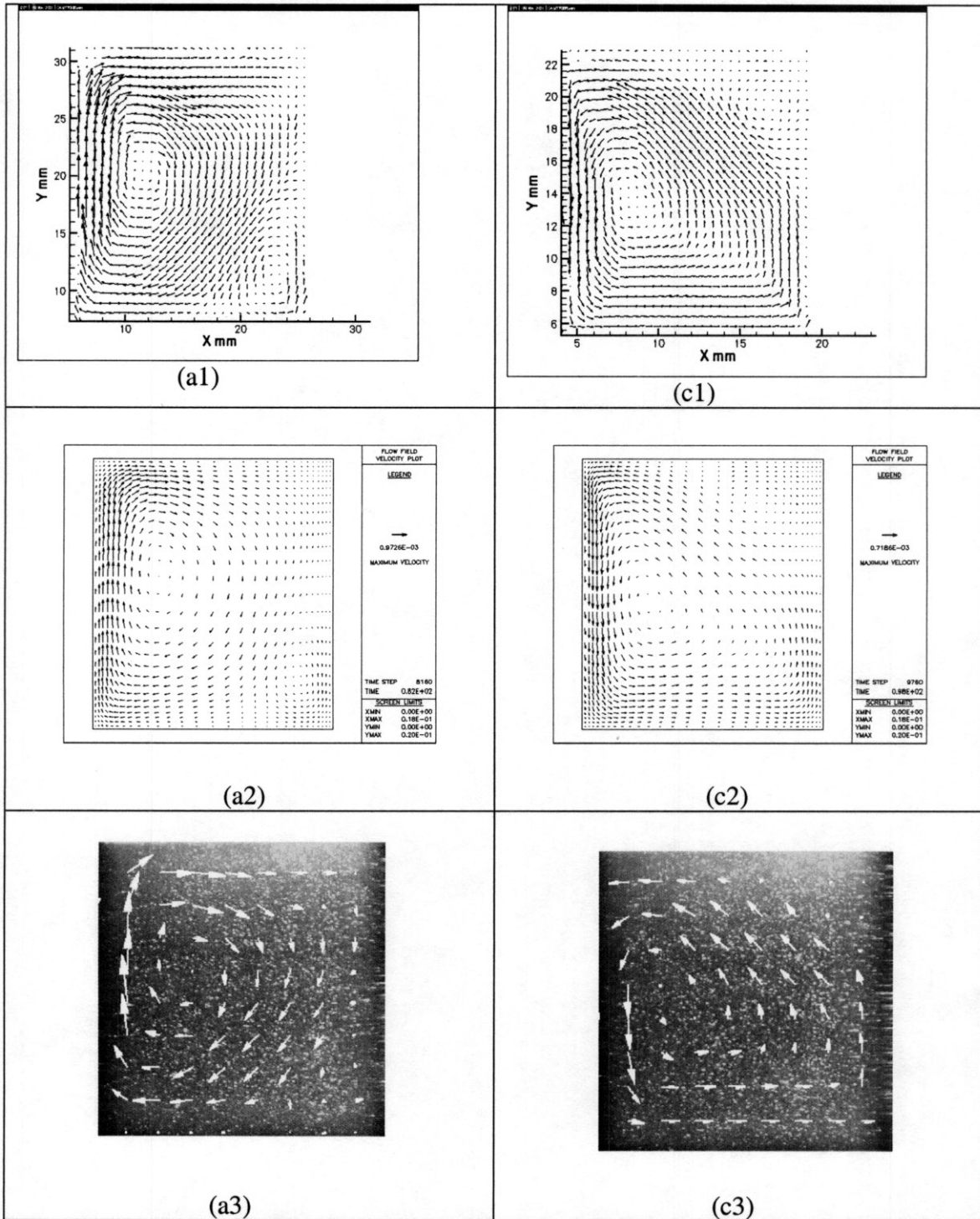


Figure 2. Oscillation of velocity fields driven by an oscillating temperature gradient within one thermal cycle, as measured by the PIV system and computed by numerical models. Frequency is 0.025Hz. (a1, c1,) are experimental results, (a2, c2) are numerical simulations and (a3, c3) are images directly from CCD camera.

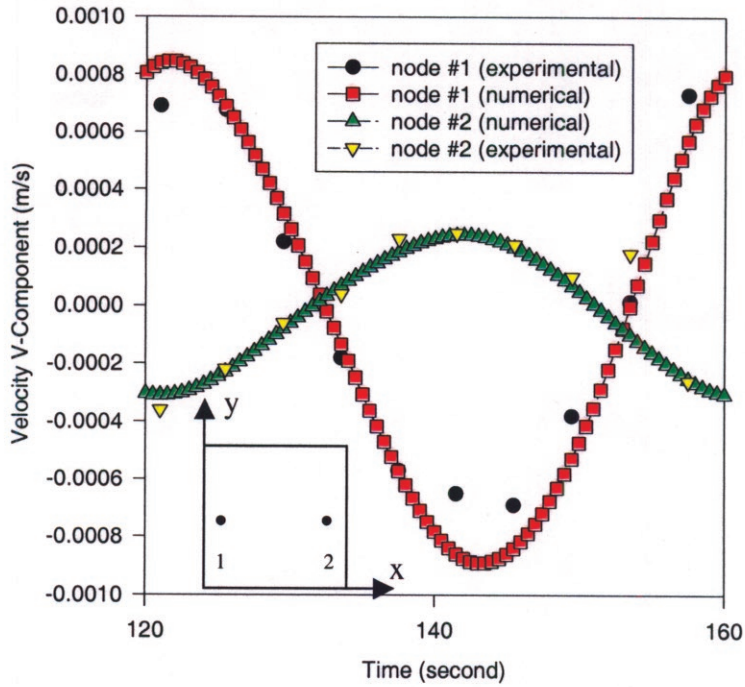


Figure 3. Comparison of measured and calculated velocity components at two locations in the testing cavity for the oscillation frequency of 0.025Hz. Coordinates of node #1 are $(x=0.0019, y=0.0105)$ and coordinate of node #2 is $(0.01601, 0.0105)$, all measured from the lower corner of the cavity.

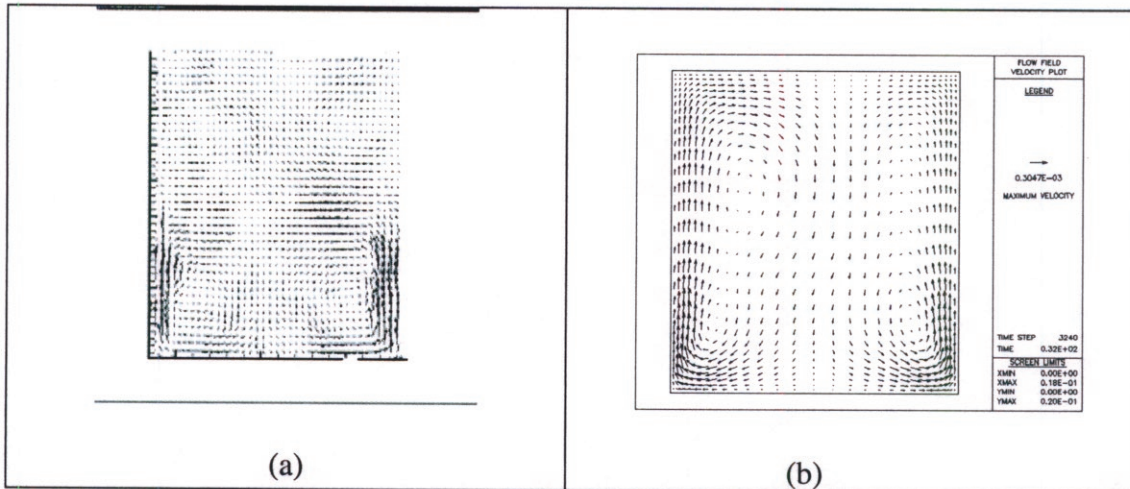


Figure 4. Experimentally measured and computed velocity field as induced by an oscillating temperature field with a frequency of 0.1Hz. (a) measured and (b) calculated.

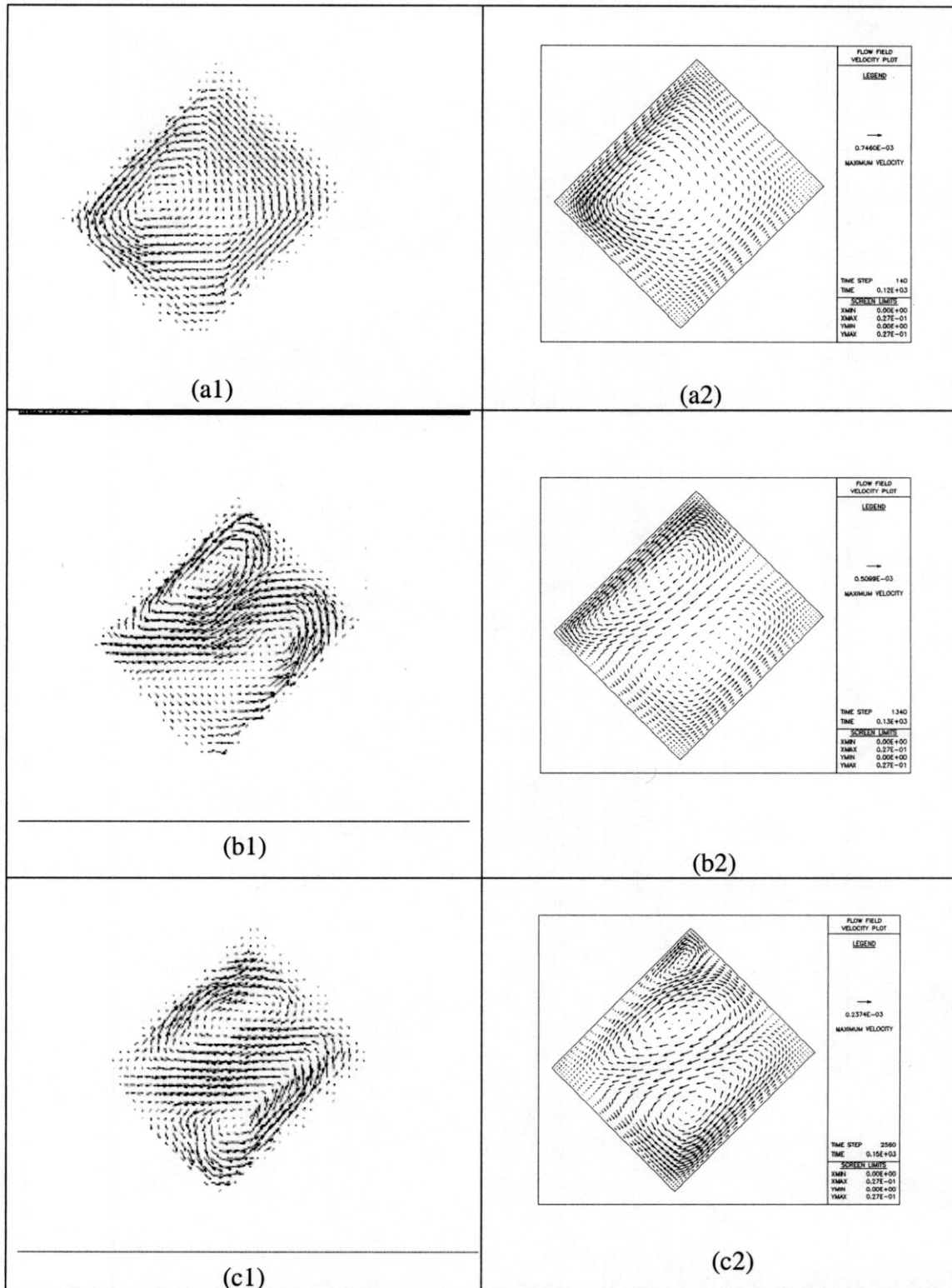


Figure 5. Comparison of transient development of oscillating velocity profiles measured by the PIV system and by the finite element model for the configuration tilted at 45° . The applied frequency is 0.025 Hz and the hot wall is on top. (a1, b1, c1) are measured and (a2, b2, c2) are numerical results.

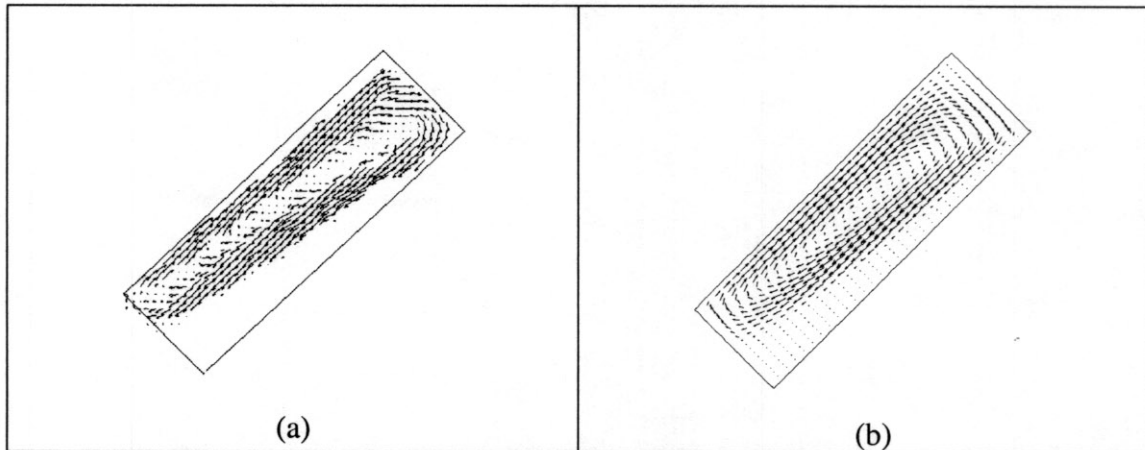


Figure 6. Comparison of measured (a) and calculated fluid field during solidification of SCN with cavity 45° tilted. Gravity points downward. The temperature of left tilt wall is 330.65 K and that at right is 335.05 K. U_{\max} of (c) is 0.7631 mm/s and U_{\max} of (d) is 0.6908 mm/s.

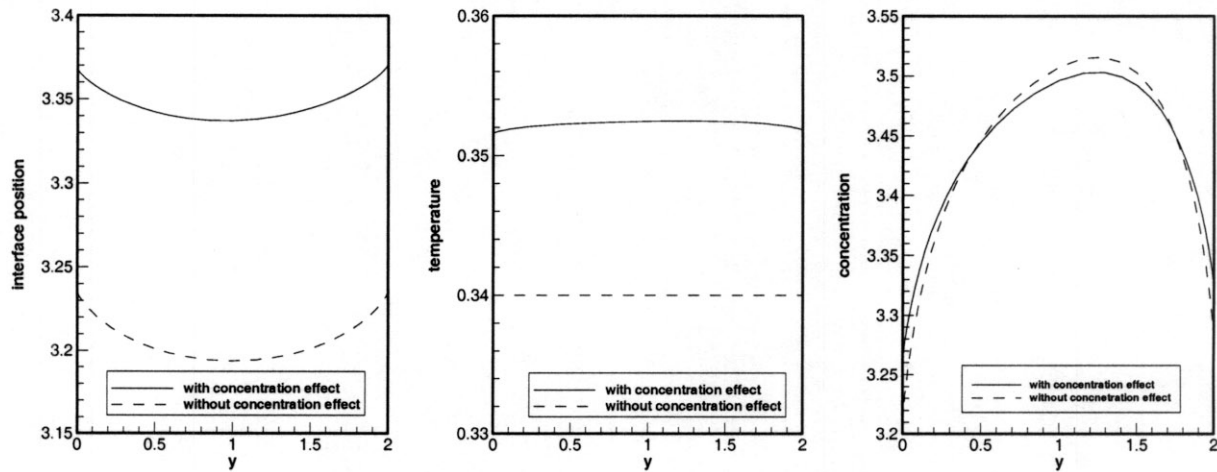


Figure 7. Dependency of interface position on concentration striation along the interface obtained from 2-D solidification model: (a) the interface positions, the temperature and concentration distributions along the growth interface of the steady cases with and without concentration effect respectively. Detailed conditions used for calculations are given in [15].

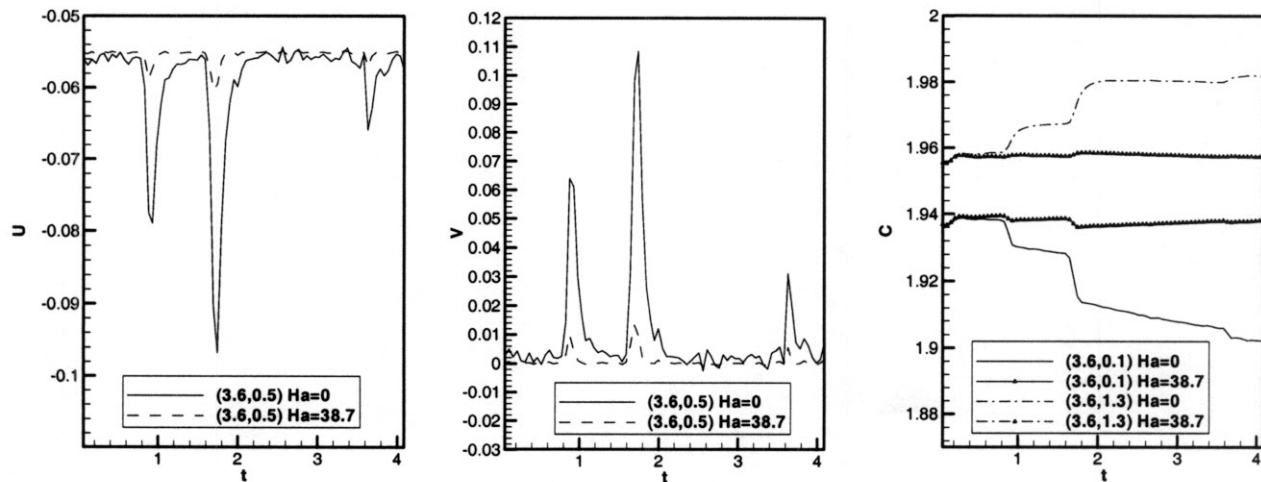


Figure 8. The effects of the magnetic field on the velocity and concentration oscillation caused by real g-jitter data at selected points in the melt near the growth front (a) $x=3.6$, $y=0.5$ (b) $x=3.6$, $y=0.5$ (c) $x=3.6$, $y=0.1$ and $x=3.6, y=1.3$. Parameters used for calculations are given in [15].

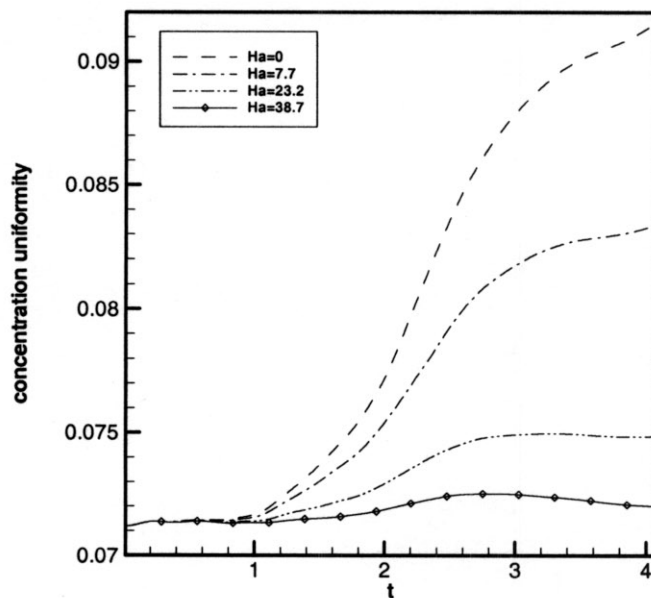


Figure 9. The effect of the magnetic field on the time evolution of the concentration uniformity along the growth interface caused by the real g-jitter. Detailed parameters for calculations are given in [15].